Quality Assurance for the Clinical Implementation of Kilovoltage Intrafraction Monitoring for Prostate Cancer VMAT

J. A. Ng[1,2], J. T. Booth[2,3], R. T. O'Brien[1], E. Colvill[1,3], C.-Y. Huang[1], P. R. Poulsen[4], and P. J. Keall[1]

1. School of Medicine, University of Sydney, NSW 2006, Australia
2. School of Physics, University of Sydney, NSW 2006, Australia
3. Northern Sydney Cancer Centre, Royal North Shore Hospital, NSW 2065, Australia
4. Department of Oncology, Aarhus University Hospital, Nørrebrogade 44, 8000 Aarhus C, Denmark

ABSTRACT

Purpose: Kilovoltage Intrafraction Monitoring (KIM) is a real-time 3D tumor monitoring system for cancer radiotherapy. KIM uses the commonly available gantry-mounted x-ray imager as input, making this method potentially more widely available than dedicated real-time 3D tumor monitoring systems. KIM is being piloted in a clinical trial for prostate cancer patients treated with VMAT (NCT01742403). The purpose of this work was to develop clinical process and quality assurance (QA) practices for the clinical implementation of KIM.

Methods: Informed by and adapting existing guideline documents from other real-time monitoring systems, KIM-specific QA practices were developed. The following five KIM-specific QA tests were included: (1) static localization accuracy, (2) dynamic localization accuracy, (3) treatment interruption accuracy, (4) latency measurement and (5) clinical conditions accuracy. Tests (1)-(4) were performed using KIM to measure static and representative patient-derived prostate motion trajectories using a 3D programmable motion stage supporting an anthropomorphic phantom with implanted gold markers to represent the clinical treatment scenario. The threshold for system tolerable latency is <1s. The tolerances for all other tests are that both the mean and standard deviation of the difference between the programmed trajectory and the measured data are <1mm. The (5) clinical conditions accuracy test compared the KIM measured positions with those measured by kV/MV triangulation from five treatment fractions acquired in a previous pilot study.

Results: For the (1) static localization, (2) dynamic localization and (3) treatment interruption accuracy tests, the mean and standard deviation of the difference is < 1.0 mm. (4) The measured latency is 350 ms. (5) For the tests with previously acquired patient data, the mean and standard deviation of the difference between KIM and kV/MV triangulation is < 1.0 mm.

Conclusions: Clinical process and QA practices for the safe clinical implementation of KIM, a novel real-time monitoring system using commonly available equipment, have been developed and implemented for prostate cancer VMAT.

I. INTRODUCTION

Tumors move during radiotherapy treatments resulting in geometric and dosimetric inaccuracies. The current proliferation of hypofractionated treatments[1] means tumor motion during treatment is becoming more significant. In order to increase dosimetric accuracy and reduce normal tissue toxicity, real-time motion adaptation strategies are needed. Real-time tumor localization modalities supply the appropriate real-time tumor positions to enable motion adaptation strategies. A variety of real-time localization modalities have been evaluated, e.g. ultrasound,[2] megavoltage (MV) imaging,[3] kV/kV triangulation,[4] kV/MV triangulation,[5] the Calypso electromagnetic (EM) tracking system,[6] MRI[7] and the Navotek radioactive fiducial tracking system.[8] However, most of these modalities are either experimental, not widely available or expensive.

A promising real-time localization modality is Kilovoltage Intrafraction Monitoring, or KIM.[9, 10] KIM measures tumor motion with the commonly available gantry-mounted x-ray imager deployed during treatment, making this method potentially more widely available than dedicated real-time 3D tumor monitoring systems. KIM has been experimentally investigated for dosimetric phantom treatments,[11, 12] and applied in non-interventional clinical prostate[13] and liver[14] cancer treatments where the acquired images were analyzed retrospectively. The resultant KIM accuracy for the clinical studies was determined to be 0.46 mm for prostate and 0.60 mm for liver. Encouraged by these results the KIM software has been refactored and enhanced for real-time operation, and a clinical trial for prostate VMAT treatments is open to accrual (NCT01742403) where the treatment will be gated if the prostate motion exceeds 3mm for more than 5 seconds.

To ensure that KIM can be used effectively and safely in a clinical environment, Quality Assurance (QA) processes for KIM are needed. The QA processes used in this study are adapted from the prescriptive QA processes developed by Santanam *et al*.[15] for another real-time localization modality, Calypso. The processes are also informed by AAPM Task Groups 104[16] and 147.[17] The four important differences between KIM and Calypso which require adapting Santanam's approach are: (1) KIM delivers kV dose to the patient while Calypso does not; (2) KIM only monitors the prostate position when the kV beam is activated while Calypso continuously monitors the prostate position; (3) KIM does not require additional equipment (assuming KIM is implemented on a linac with an existing gantry-mounted kV imager); and (4) KIM does not require a dedicated couch.

The aim of this study is to describe the QA processes for KIM that will be used for the first time in a prospective clinical trial for prostate cancer.

II. METHODS AND MATERIALS

II.A. The Kilovoltage Intrafraction Monitoring system

Figure 1 shows the clinical process workflow for KIM with radiation beam gating, henceforth referred to as KIM gating.

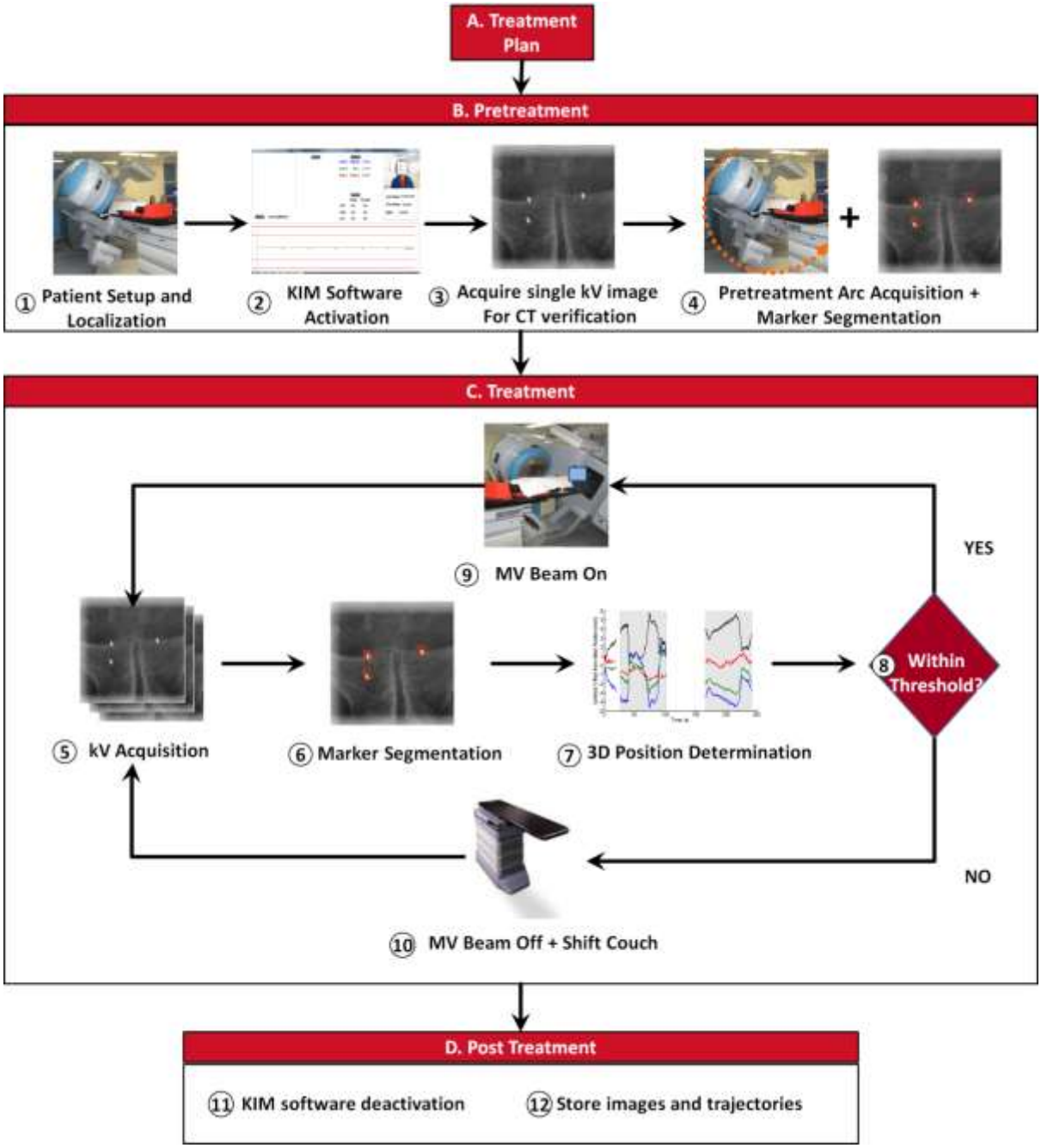

Figure 1. The clinical process workflow for Kilovoltage Intrafraction Monitoring gating.

A standard computed tomography (CT) scan for the patient is acquired. The treatment plan is created ensuring that the treatment isocenter is placed at the geometric center of the center of the three fiducial markers (Figure 1-A). This step involves some uncertainty due to the CT

reconstruction of the markers, which gives uncertainty in the size and center of the markers. Note that because of the varying volume of the markers, the isocenter is placed at the geometric center of the marker centers, which will be different from the center of mass if the marker images have different volumes. Prior to treatment, the patient is localized via kV/kV match or cone beam computed tomography (CBCT) (Figure 1-1). The KIM software is activated (Figure 1-2) and a single kV image is acquired to determine if the present marker positions match the CT scan marker positions (Figure 1-3). A 120° pretreatment arc is then acquired and the markers in these images segmented (Figure 1-4) to build a probability density function (pdf) required for the KIM 3D trajectory determination[10] with real-time 3D trajectories displayed after 40° of gantry rotation. The pdf is built using with the most recent 500 images. To improve the marker segmentation performance, the most recent 3 frames are averaged. The pdf is updated after every new image has been acquired. These values were determined by running the code with various settings using prior image data[13] to find a set of values that performed well across the range of clinical variation observed to date. The parameter values are user-configurable.

During MV beam on, kV images of the prostate are acquired at a frequency of 5 or 10 Hz (Figure 1-5). The KIM software segments the markers in each new image to determine the 2D marker positions (Figure 1-6). These 2D marker positions are converted to 3D positions via a specialized mathematical algorithm developed by Poulsen *et al.*[10] (Figure 1-7). Based on whether any of the LR, SI or AP positions (Figure 1-8) of the prostate has exceeded a preset threshold (e.g. 3 mm for 5 s) (Figure 1-8), it is decided whether to continue treatment (Figure 1-9) or pause the MV treatment beam and shift the couch (Figure 1-10). If the kV beam is paused, e.g. during a couch shift, then images are briefly acquired to determine if the prostate is still within tolerance. This process is repeated until the treatment is complete.

Post treatment, the KIM software is deactivated and the acquired data are saved for analysis (Figure 1-11 and 12).

II.B. Quality assurance tests for KIM

The QA tests for the Calypso electromagnetic (EM) system by Santanam *et al*.[15] were adapted for the KIM QA tests. Several of the Santanam QA tests for Calypso did not need to be performed for KIM as they are part of an existing kV imager QA process.[18] For example, the camera and system calibration are adapted to KIM as the TG 142 'Imaging and treatment coordinate coincidence test' and do not need to be repeated for the KIM-specific tests. The TG 142 image quality tests are also important to follow if using kV imagers for KIM.

For all of the geometric tests, the pass criterion of 1.0 mm was applied to the mean and standard deviation of the KIM-measured to the ground truth. The 1 mm value was chosen so that the error from the KIM measurement was well below typical margins for prostate radiotherapy, and in line with other geometric errors from e.g. isocenter calibration, kV alignment and couch tolerance.[18] Improvements below 1 mm are of limited practical value as this is within typical linac specifications. The 1 second latency tolerance was chosen as a value that would allow detection and correction on a timescale that is small with respect to typical prostate motion.

As KIM relies either on the correlation of internal motion in the observed (perpendicular to the kV x-ray beam in any given projection) and unobserved (parallel to the x-ray beam) dimensions or confinement of motion in one or more directions, a programmable motion phantom reproducing patient-measured prostate motion trajectories is necessary for quality assurance. For these measurements we adapted the HexaMotion (Scandidos) platform to accommodate a pelvic Rando phantom (The Phantom Laboratory, Salem, NY) with implanted markers (Figure 2). The HexaMotion platform has been evaluated previously to reproduce prostate trajectories with high fidelity, better than 0.5mm.[19] The tests were performed using a CT scan and treatment plan of the Rando phantom, and therefore the results represent end-to-end tests.

II.B.1 Static localization accuracy

The static localization accuracy tests are used to assess whether KIM can determine static positions accurately and determine the direction of static shifts correctly to ensure the KIM and patient co-ordinate systems are the same. A Rando phantom was implanted with 3 gold fiducial markers (1.2 mm diameter × 3.0 mm length) in a position mimicking the prostate position and a CT scan acquired with 2mm slice width. A VMAT treatment plan was created.

The phantom was placed with the setup as shown in Figure 2. A kV/kV localization pair was used to align the marker geometric center to isocenter. KIM was applied with an imaging

frequency of 10 Hz to determine the trajectory of the static phantom for a 120° pretreatment arc and one treatment arc for each of seven phantom positions: the phantom at the isocenter, and also shifted ±5 mm from the initial position along individual cardinal axes (in the ± left-right (LR), anterior-posterior (AP) and superior-inferior (SI) directions). The accuracy of the determination of the static phantom position was measured against the known shift and correctness of the directions of these shifts was assessed.

We calculated the mean difference between measured and programmed trajectories, the standard deviation, and the 5^{th} and 95^{th} percentile.

Figure 2. Setup of the Rando phantom for the QA tests. The Rando phantom was placed on an in-house modified wooden platform mounted to the HexaMotion. The HexaMotion translates the Rando phantom with programmed prostate trajectories during irradiation.

II.B.2 Dynamic localization accuracy

Dynamic localization refers to the accuracy of KIM determined trajectories and was assessed against the programmed 3D prostate trajectory of the HexaMotion (Figure 3). The HexaMotion was programmed to move with six 'typical' prostate trajectories as measured from prostate patients in a clinical study by Langen *et al.*[20] These trajectories include; stable trajectory, continuous drift, persistent excursion, transient excursion, high-frequency excursion, and erratic behavior. No gating tolerance was applied and these trajectories were completed without treatment interruption. It is important to note that the KIM results will be trace dependent: in a simulation study over the Langen database the mean 3D root-mean-square (rms) error was 0.22 mm, 0.8% of the traces had rms errors >1 mm.[9] The experimental measurement errors are expected to be larger than the simulation errors.

General prostate motion trends include low LR motion,[6, 10, 21] and a positive correlation between SI and AP motion.[6, 10, 22, 23] The underlying principle of KIM is that it relies on the correlation of motion of internal anatomy in different directions and also finds out (and exploits) if motion is small. For prostate, this correlation of motion is limited to SI and AP motion correlation.[10] Hence, patient trajectories, rather than artificial trajectories are needed for the dynamic localization and treatment interruption accuracy tests.

II.B.3 Treatment interruption accuracy

The treatment interruption accuracy test determines how accurately KIM can monitor the actual target motion under the clinically realistic situation where a position threshold has been exceeded during treatment and a couch shift performed, following the Figure 1 workflow. The accuracy will be limited by the inherent uncertainty in remote couch shifts, estimated at 0.5mm for the Exact Couch (Varian). The treatment interruption tests were performed with the same setup in Figure 2 and method of dynamic localization with the gating tolerance of 3mm/5s applied. That is, if any of the LR, AP and/or SI trajectories exceed 3.0 mm from the isocenter for 5.0 s, the MV and kV beams are manually paused. The couch is shifted remotely so that the target moves back to isocenter. kV imaging is then acquired for 5 seconds to ensure that the target position remains within the 3mm/5s tolerance. If this condition is not met, another couch shift is performed (Figure 1-10). Following that, treatment with KIM is resumed. The couch shifts are logged each time they are made.

For each of the trajectories with couch shifts we calculated the mean difference between measured and programmed trajectories (including shifts), the standard deviation, and the 5^{th} and 95^{th} percentile.

II.B.4 Latency measurement

Measurement of the latency for KIM is important to ensure that positions of high velocity targets can be determined. The latency is defined as the time delay between when a target moves and when KIM resolves the motion. An indirect measurement of latency for KIM was performed using the Calypso electromagnetic tracking system. The HexaMotion was programmed to move with a superior-inferior sinusoidal motion of period 4 s and peak to peak amplitude 10 mm. Calypso beacons were placed on the Rando phantom for tracking.

Calypso and KIM both localized the phantom position in ‘real-time’ during treatment. Video images (at 30 Hz) were acquired of the KIM and Calypso output screens together. The SI positions from each system were determined and plotted. A sine curve was fitted to each

plot and the time difference between these two sine curves was calculated. The KIM latency is the sum of the measured time difference and the measured Calypso (with MLC tracking) latency of 230 ms.[24] Note that alternate methods of measuring latency exist, for example a measurement using a dial indicator, or using the RPM. The Calypso (with MLC tracking) was the simplest at our institution, and represents the upper bound of the latency measurement as the additional MLC tracking response time (estimated at ~80 ms) is not subtracted.

II.B.5 Clinical conditions accuracy

The previously described tests were performed on phantoms. A comparison of KIM and kV/MV triangulation from previously treated patients provides a measure of the accuracy of KIM under clinical conditions.[13] This test was performed to benchmark KIM following the real-time refactoring of the retrospective version of the software used in the pilot study.[13] The markers were manually segmented in MV images acquired for five fractions to obtain their 2D positions. The 2D MV positions were triangulated with the 2D positions from kV images acquired at the same time to obtain the 3D positions of the markers. The mean difference and standard deviation of the difference between KIM and kV/MV triangulated trajectories were computed for those five fractions, with the kV/MV triangulated trajectories assumed to be the ground truth.

III. RESULTS

III.A. Static localization accuracy

Table I shows the static localization test results. The mean difference and standard deviation of the difference criteria pass for each direction for all scenarios. The directions of the shifts are also correct.

Table I. Static localization test results.

Phantom Shift	Direction	Mean difference (mm) (Required: < 1.0 mm)	Standard deviation (mm) (Required: < 1.0 mm)	Percentiles (5%, 95%)
None	LR	0.06	0.15	(-0.23, 0.21)
	SI	-0.46	0.08	(-0.58, -0.30)
	AP	0.24	0.19	(-0.17, 0.52)
5 mm left	LR	0.23	0.13	(-0.02, 0.37)
	SI	0.61	0.07	(0.49, 0.77)

	AP	0.20	0.20	(-0.22, 0.50)
5 mm right	LR	0.44	0.17	(0.09, 0.60)
	SI	0.63	0.07	(0.52, 0.77)
	AP	0.21	0.22	(-0.27, 0.53)
5 mm superior	LR	0.07	0.15	(-0.24, 0.21)
	SI	-0.34	0.07	(-0.46, -0.23)
	AP	0.21	0.18	(-0.16, 0.50)
5 mm inferior	LR	0.06	0.19	(-0.33, 0.23)
	SI	-0.09	0.08	(-0.21, 0.04)
	AP	0.25	0.21	(-0.15, 0.59)
5 mm anterior	LR	-0.12	0.15	(-0.42, 0.04)
	SI	0.61	0.08	(0.51, 0.76)
	AP	0.30	0.25	(-0.22, 0.62)
5 mm posterior	LR	-0.15	0.20	(-0.56, 0.02)
	SI	0.60	0.07	(0.48, 0.72)
	AP	0.31	0.20	(-0.12, 0.64)

III.B. Dynamic localization accuracy

Figure 3 shows the plots of the dynamic localization measurements with KIM. For each motion type, the KIM (measured) trajectory was overlaid on the HexaMotion (actual) trajectory. The HexaMotion trajectory was initiated at the beginning of the pretreatment arc. In Figure 3, the time axis is started 10s before treatment. The grey shading highlights when treatment is being delivered. As the SI position is always perpendicular to the imager, we expect SI errors to be low. Errors in the AP and LR directions will be dependent on the gantry angle (whether the motion is being directly measured or inferred), the underlying correlation of motion in the different directions for the patient and noise of the input trace.

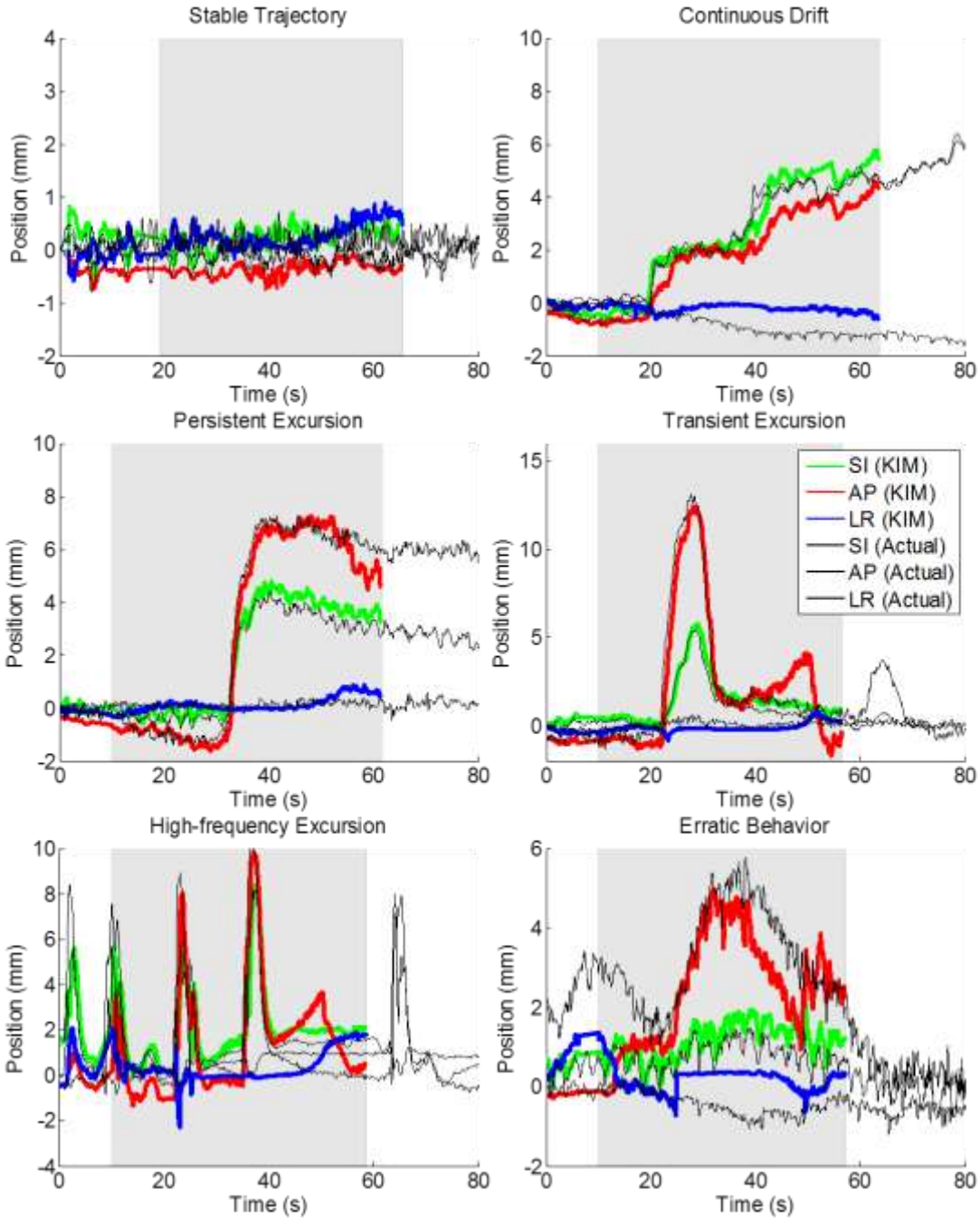

Figure 3. Dynamic localization trajectories. Top left: stable trajectory. Top right: continuous drift. Center left: persistent excursion. Center right: high-frequency excursion. Bottom left: transient excursion. Bottom right: erratic behavior. Time 0 corresponds to 10s before the start of treatment. The gray shading indicates when the MV treatment beam is on.

Table II summarizes the dynamic localization test results as mean difference between KIM and HexaMotion, standard deviation of the difference, and the 5th and 95th percentiles. These metrics were computed when the treatment beam was on. The pass criterion for the mean difference is values less than 1.0 mm. The pass criterion for the standard deviation of the

difference is also values less than 1.0 mm. The percentiles are shown to provide further detail on the positional accuracy.

Table II. Dynamic localization test results.

Motion Type	Direction	Mean difference (mm) (Required: < 1.0 mm)	Standard deviation (mm) (Required: < 1.0 mm)	Percentiles (5%, 95%)
Stable	LR	0.53	0.27	(0.13, 0.97)
	SI	0.87	0.10	(0.71, 1.04)
	AP	0.08	0.23	(-0.29, 0.44)
Continuous	LR	0.50	0.19	(0.11, 0.79)
	SI	0.58	0.35	(-0.03, 1.12)
	AP	-0.07	0.35	(-0.67, 0.47)
Persistent Excursion	LR	-0.48	0.27	(-0.88, -0.02)
	SI	0.27	0.17	(0.01, 0.55)
	AP	-0.14	0.30	(-0.59, 0.37)
High-frequency Excursion	LR	0.54	0.20	(0.35, 1.03)
	SI	0.81	0.31	(0.55, 1.16)
	AP	-0.04	0.74	(-0.92, 1.63)
Transient Excursion	LR	-0.09	0.22	(-0.51, 0.21)
	SI	0.33	0.19	(0.04, 0.59)
	AP	-0.09	0.67	(-1.41, 1.14)
Erratic Behavior	LR	0.06	0.44	(-0.68, 0.68)
	SI	0.32	0.26	(-0.06, 0.75)
	AP	-0.14	0.97	(-1.89, 1.42)

III.C. Treatment interruption accuracy

Figure 4 shows the plots of the treatment interruption accuracy test measurements. Four of the 6 trajectories exceeded the 3 mm /5 s gating threshold and were used because a gating event occurred. The KIM measured trajectory is overlaid on the HexaMotion (programmed) trajectory.

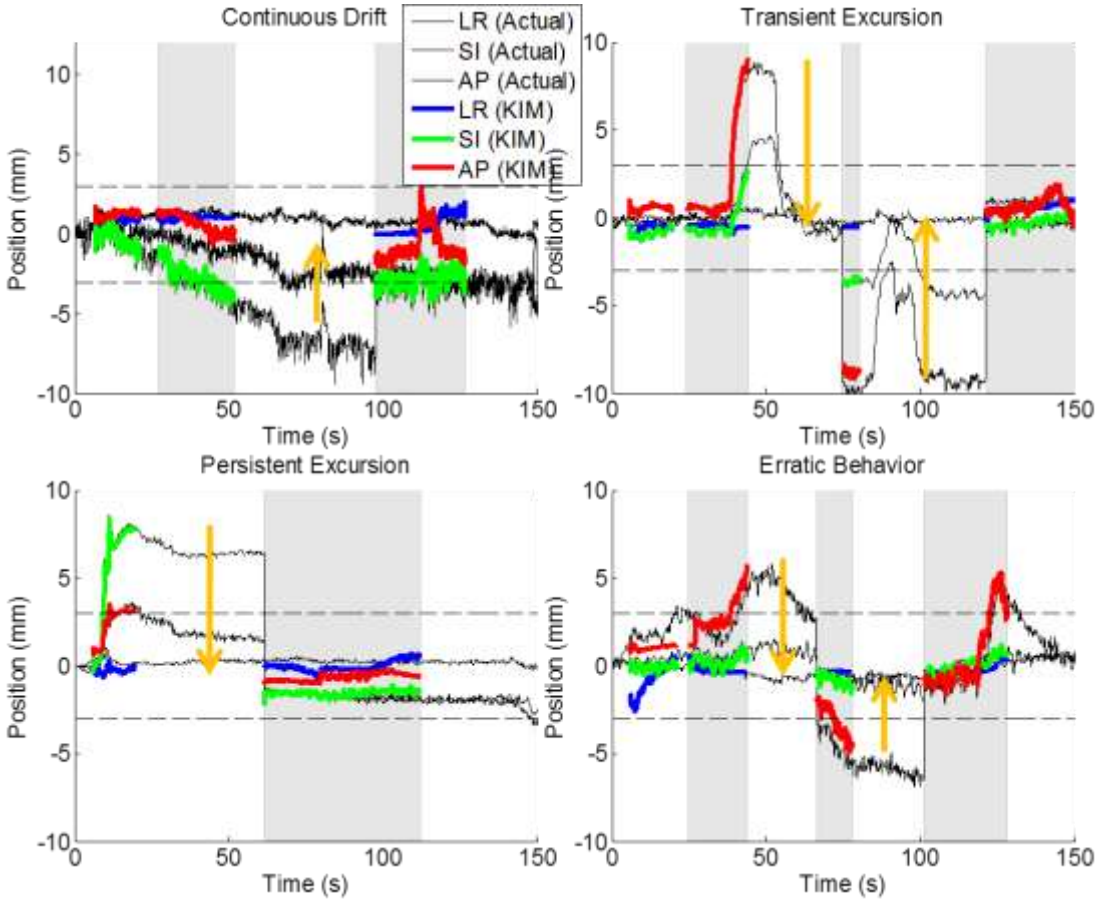

Figure 4. Trajectories for the treatment interruption test. Shifts were applied to the actual trajectories. Top left: continuous drift demonstrating a single interruption and couch shift during treatment. Top right: transient excursion demonstrating a couch shift during treatment, that had to be re-corrected before treatment resumption due to further prostate motion. Bottom left: persistent excursion demonstrating a couch shift required before treatment. Bottom right: erratic behavior that also had to be re-corrected before treatment resumption. The gray shading indicates when the treatment beam is on. The orange arrow represents approximately where the couch shift occurred.

Table III shows the treatment interruption accuracy test results. The mean difference and standard deviation of the difference criteria pass for each direction for all scenarios.

Table III. Treatment interruption test results.

Scenario	Direction	Mean difference (mm) (Required: < 1.0 mm)	Standard deviation (mm) (Required: < 1.0 mm)	Percentiles (5%, 95%)

Continuous	LR	0.18	0.21	(-0.23, 0.45)
	SI	0.04	0.33	(-0.42, 0.58)
	AP	0.15	0.42	(-0.49, 0.84)
Persistent Excursion	LR	0.23	0.44	(-0.70, 0.95)
	SI	0.50	0.11	(0.33, 0.69)
	AP	-0.32	0.43	(-0.91, 0.34)
Transient Excursion	LR	0.06	0.24	(-0.50, 0.33)
	SI	0.74	0.39	(-0.03, 1.26)
	AP	-0.23	0.84	(-1.49, 0.96)
Erratic Behavior	LR	0.35	0.43	(-0.48, 0.85)
	SI	0.61	0.26	(0.20, 1.06)
	AP	-0.49	0.81	(-1.96, 0.70)

III.D. Latency measurement

The time difference between the KIM and Calypso fitted sine curves was measured to be 120 ms. Adding the time difference to the measured Calypso latency of 230 ms produces a KIM latency of 350 ms. This value is an upper bound as the Calypso measurements include the additional time needed for MLC tracking, and also the KIM latency could be reduced by improved image handling and code optimization. The measured KIM latency is well below the set tolerance of 1 s determined for prostate real-time localization.

III.E. Clinical conditions accuracy

Table IV shows the comparison of KIM and kV/MV triangulation for the 5 patient fractions of MV images. The mean difference and standard deviation of the difference criteria pass for each direction for all scenarios.

Table IV. An accuracy comparison of KIM compared with kV/MV triangulation from previously acquired clinical data.

Patient/ Fraction	No. of MV images	Direction	Mean difference (mm) (Required: < 1.0 mm)	Standard deviation (mm) (Required: < 1.0 mm)	Percentiles (5%, 95%)
6/40	12	LR	0.55	0.08	(0.37, 0.70)
		SI	0.16	0.08	(-0.03, 0.25)

		AP	-0.14	0.35	(-0.55, 0.39)
8/37	32	LR	0.03	0.36	(-0.70, 1.00)
		SI	-0.52	0.31	(-1.10, 0.10)
		AP	0.78	0.88	(-0.80, 2.40)
9/20	264	LR	0.07	0.64	(-0.75, 1.24)
		SI	0.28	0.19	(-0.03, 0.57)
		AP	008	0.54	(-0.70, 1.13)
9/36	88	LR	-0.08	0.34	(-0.80, 0.80)
		SI	-0.75	0.31	(-1.30, -0.10)
		AP	0.89	0.45	(-0.10, 1.90)
10/39	23	LR	0.58	0.16	(0.33, 0.84)
		SI	0.19	0.17	(-0.08, 0.49)
		AP	-0.17	0.21	(-0.48, 0.24)

III.F. Summary

Table V shows the summary of all the QA tests performed. All required tests passed. The proposed test frequency is based on TG 147 recommendations.[17] Although TG 147 is based on non-radiographic systems, it encompasses the QA of a real-time localization modality which can be applied other real-time methods.

We stress that these QA tests should need to be performed in concert with, and do not replace, kV imaging system tests, as described in TG 142.[18]

Table V. Summary of QA tests and proposed test frequency.

Test	Frequency	Subtest	Pass Criteria
1. Static localization accuracy	Annual[&] & monthly	a. Mean difference	< 1.0 mm
		b. Standard deviation of differences	< 1.0 mm
		c. Directionality	Correct
2. Dynamic localization accuracy	Annual & monthly[*]	a. Mean difference	< 1.0 mm
		b. Standard deviation of differences	< 1.0 mm
3. Treatment interruption	Annual & monthly[*]	a. Mean difference	< 1.0 mm

accuracy		b. Standard deviation of differences	< 1.0 mm
4. Latency measurement	Annual		< 1.0 s

[&]Annual tests should also be performed as part of commissioning, and after any software changes.

[*]For monthly quality assurance, single rather than multiple motion traces can be used, with a set schedule to cycle through different motion traces (c.f. AAPM TG 135[25] end-to-end monthly tests).

IV. DISCUSSION

The QA tests in this study were designed with the framework outlined in Santanam *et al*. which focused on the QA of the Calypso electromagnetic system, which is also a real-time localization modality. The QA tests which are similar between KIM and Santanam include static localization accuracy, dynamic localization accuracy and latency measurement. Additional QA tests over those developed in Santanam are the tests with previously acquired clinical data (MV/KV triangulation), and the treatment interruption tests. The tests with previously acquired patient data were necessary to gauge the fidelity of KIM with real data. The treatment interruption accuracy tests were needed as they are unique to the KIM gating implementation which requires remote couch shifts. Separate QA to assess the accuracy of the couch shifts is outlined in TG 142, in which the couch tolerance is suggested to be (± 2 mm / 1°).[18]

The QA for the Cyberknife, a robotic radiosurgery system which also adapts to real-time tumor motion was outlined by Dieterich *et al*.[25] While the scope of the Cyberknife QA is comprehensive and includes the entire radiosurgery system, similarities with the current study include the assessment of the geometric accuracy.

KIM delivers kV dose to the patient. The assessment of dose is important as part of the QA of the real-time KIM system. However, KIM dose was measured in a previous study hence, the dose assessment is not included in this study. Typically, a single 6 cm × 6 cm projection delivers 1 μSv of dose.[26] The 6 cm × 6 cm field size was selected based on the quantification of the field sizes needed to image the implanted markers through a review of 22 prostate patient CT images.[27]

Several strategies for the dose reduction with KIM were identified and will be implemented when possible. These include:

- Reducing the MV scatter by reading out the imaging panel prior to acquiring the kV image. This allows the kV frame rate to be reduced.[13]
- Temporarily halting the MV beam during kV acquisition as proposed by Ling *et al*.[28]
- Utilizing patient and gantry angle specific field sizes.[13]
- Varying the exposure with gantry angle. At present, the same exposure parameters are used for all gantry angles. This means a higher than necessary dose is delivered for AP projections. Using the CT analogy of automatic brightness control can further reduce the dose.[13]
- Incorporating the imaging dose into the optimization framework to reduce delivery time where beneficial.[29]

It should also be noted that if KIM replaces daily cone beam CT imaging, then the total imaging dose to the patient would be reduced.

Several aspects of the KIM gating workflow can be improved. Currently, the radiation beam is manually switched off based on a visual signal from the KIM user interface. The couch shift is also manually performed. Both of these manual steps could be easily automated, however they involve a level of integration with the linac that would require an extra level of regulatory review.

V. CONCLUSION

Clinical process and QA practices for the safe clinical implementation of KIM, a novel real-time monitoring system using commonly available equipment, have been developed and implemented for prostate cancer VMAT. A prospective clinical trial of KIM is actively recruiting prostate cancer patients.

ACKNOWLEDGEMENTS

The authors acknowledge funding from the Australian National Health and Medical Research Council and Cancer Australia. We thank Richard Speight for independent review and clinical insight into the KIM process. We thank our European and US collaborators who have given us independent review and feedback of the KIM QA process through web-conferences. Julie Baz improved the clarity of the manuscript. Varian Medical Systems is acknowledged for

providing the use of the iTools Capture software and associated hardware to allow image streaming from the OBI to the KIM software.

REFERENCES

[1] H. Pan, D.R. Simpson, L.K. Mell, A.J. Mundt, J.D. Lawson, "A survey of stereotactic body radiotherapy use in the United States," Cancer **117**, 4566-4572 (2011).

[2] J. Schlosser, K. Salisbury, D. Hristov, "Telerobotic system concept for real-time soft-tissue imaging during radiotherapy beam delivery," Med Phys **37**, 6357-6367 (2010).

[3] R.I. Berbeco, F. Hacker, D. Ionascu, H.J. Mamon, "Clinical Feasibility of Using an EPID in cine Mode for Image-Guided Verification of Stereotactic Body Radiotherapy," International Journal of Radiation Oncology* Biology* Physics **69**, 258-266 (2007).

[4] H. Shirato, S. Shimizu, T. Kunieda, K. Kitamura, M. van Herk, K. Kagei, T. Nishioka, S. Hashimoto, K. Fujita, H. Aoyama, K. Tsuchiya, K. Kudo, K. Miyasaka, "Physical aspects of a real-time tumor-tracking system for gated radiotherapy," International Journal of Radiation Oncology, Biology, Physics **48**, 1187-1195 (2000).

[5] B. Cho, P.R. Poulsen, A. Sloutsky, A. Sawant, P.J. Keall, "First Demonstration of Combined kV/MV Image-Guided Real-Time Dynamic Multileaf-Collimator Target Tracking," International journal of radiation oncology, biology, physics **74**, 859-867 (2009).

[6] P. Kupelian, T. Willoughby, A. Mahadevan, T. Djemil, G. Weinstein, S. Jani, C. Enke, T. Solberg, N. Flores, D. Liu, D. Beyer, L. Levine, "Multi-institutional clinical experience with the Calypso System in localization and continuous, real-time monitoring of the prostate gland during external radiotherapy," International journal of radiation oncology, biology, physics **67**, 1088-1098 (2007).

[7] S.P.M. Crijns, B.W. Raaymakers, J.J.W. Lagendijk, "Proof of concept of MRI-guided tracked radiation delivery: tracking one-dimensional motion," Physics in medicine and biology **57**, 7863 (2012).

[8] T. Shchory, D. Schifter, R. Lichtman, D. Neustadter, B.W. Corn, "Tracking Accuracy of a Real-Time Fiducial Tracking System for Patient Positioning and Monitoring in Radiation Therapy," International journal of radiation oncology, biology, physics **78**, 1227-1234 (2010).

[9] P.R. Poulsen, B. Cho, P.J. Keall, "Real-time prostate trajectory estimation with a single imager in arc radiotherapy: a simulation study," Physics in Medicine and Biology **54**, 4019 (2009).

[10] P.R. Poulsen, B. Cho, K. Langen, P. Kupelian, P. Keall, "Three-dimensional prostate position estimation with a single x-ray imager utilizing the spatial probability density," Physics in Medicine and Biology **53**, 4331-4353 (2008).

[11] P.R. Poulsen, B. Cho, D. Ruan, A. Sawant, P.J. Keall, "Dynamic multileaf collimator tracking of respiratory target motion based on a single kilovoltage imager during arc radiotherapy," International journal of radiation oncology, biology, physics **77**, 600-607 (2010).

[12] P.R. Poulsen, B. Cho, A. Sawant, P.J. Keall, "Implementation of a new method for dynamic multileaf collimator tracking of prostate motion in arc radiotherapy using a single kV imager," International journal of radiation oncology, biology, physics **76**, 914-923 (2010).

[13] J.A. Ng, J.T. Booth, P.R. Poulsen, W. Fledelius, E.S. Worm, T. Eade, F. Hegi, A. Kneebone, Z. Kuncic, P.J. Keall, "Kilovoltage Intrafraction Monitoring for Prostate Intensity Modulated Arc Therapy: First Clinical Results," International Journal of Radiation Oncology, Biology, Physics **84**, e655-e661 (2012).

[14] E.S. Worm, M. Høyer, W. Fledelius, P.R. Poulsen, "Three-dimensional, Time-Resolved, Intrafraction Motion Monitoring Throughout Stereotactic Liver Radiation Therapy on a Conventional Linear Accelerator," Int. J. Radiat. Oncol. Biol. Phys. **86**, 190-197 (2013).

[15] L. Santanam, C. Noel, T.R. Willoughby, J. Esthappan, S. Mutic, E.E. Klein, D.A. Low, P.J. Parikh, "Quality assurance for clinical implementation of an electromagnetic tracking system," Medical Physics **36**, 3477-3486 (2009).
[16] Y. Fang-Fang, W. John, "Report of Task Group 104 of the Therapy Imaging Committee AAPM," AAPM2009).
[17] T. Willoughby, J. Lehmann, J.A. Bencomo, S.K. Jani, L. Santanam, A. Sethi, T.D. Solberg, W.A. Tomé, T.J. Waldron, "Quality assurance for nonradiographic radiotherapy localization and positioning systems: Report of Task Group 147," Medical Physics **39**, 1728-1747 (2012).
[18] E.E. Klein, J. Hanley, J. Bayouth, F.-F. Yin, W. Simon, S. Dresser, C. Serago, F. Aguirre, L. Ma, B. Arjomandy, C. Liu, C. Sandin, T. Holmes, "Task Group 142 report: Quality assurance of medical acceleratorsa)," Medical Physics **36**, 4197-4212 (2009).
[19] P. Satory, A. Rice, J.-A. Ng, J.T. Booth, "Commissioning the Delta4 Hexamotion 6D motion jig (abstract)," Engineering and Physical Sciences in Medicine Conference2013).
[20] K.M. Langen, T.R. Willoughby, S.L. Meeks, A. Santhanam, A. Cunningham, L. Levine, P.A. Kupelian, "Observations on Real-Time Prostate Gland Motion Using Electromagnetic Tracking," International journal of radiation oncology, biology, physics **71**, 1084-1090 (2008).
[21] P. Cheung, K. Sixel, G. Morton, D.A. Loblaw, R. Tirona, G. Pang, R. Choo, E. Szumacher, G. DeBoer, J.-P. Pignol, "Individualized planning target volumes for intrafraction motion during hypofractionated intensity-modulated radiotherapy boost for prostate cancer," International Journal of Radiation Oncology, Biology, Physics **62**, 418-425 (2005).
[22] P.R. Poulsen, L.P. Muren, M. Hoyer, "Residual set-up errors and margins in on-line image-guided prostate localization in radiotherapy," Radiother Oncol **85**, 201-206 (2007).
[23] G. Soete, M. De Cock, D. Verellen, D. Michielsen, F. Keuppens, G. Storme, "X-ray–assisted positioning of patients treated by conformal arc radiotherapy for prostate cancer: Comparison of setup accuracy using implanted markers versus bony structures," International Journal of Radiation Oncology, Biology, Physics **67**, 823-827 (2007).
[24] P.J. Keall, E. Colvill, R. O'Brien, J.A. Ng, P.R. Poulsen, T. Eade, A. Kneebone, J.T. Booth, "The first clinical implementation of electromagnetic transponder-guided MLC tracking," Med Phys **41**, 020702 (2014).
[25] S. Dieterich, C. Cavedon, C.F. Chuang, A.B. Cohen, J.A. Garrett, C.L. Lee, J.R. Lowenstein, M.F. d'Souza, D.D. Taylor, X. Wu, C. Yu, "Report of AAPM TG 135: Quality assurance for robotic radiosurgery," Medical Physics **38**, 2914-2936 (2011).
[26] J.A. Ng, J. Booth, P. Poulsen, Z. Kuncic, P.J. Keall, "Estimation of effective imaging dose for kilovoltage intratreatment monitoring of the prostate position during cancer radiotherapy," Physics in Medicine and Biology **58**, 5983 (2013).
[27] K.C. James, N. Jin Aun, J.K. Paul, T.B. Jeremy, "Measurement of patient imaging dose for real-time kilovoltage x-ray intrafraction tumour position monitoring in prostate patients," Physics in Medicine and Biology **57**, 2969 (2012).
[28] C. Ling, P. Zhang, T. Etmektzoglou, J. Star-lack, M. Sun, E. Shapiro, M. Hunt, "Acquisition of MV-scatter-free kilovoltage CBCT images during RapidArc™ or VMAT," Radiotherapy and Oncology **100**, 145-149 (2011).
[29] Z. Grelewicz, R.D. Wiersma, "Combined MV+ kV inverse treatment planning for optimal kV dose incorporation in IGRT," Physics in medicine and biology **59**, 1607 (2014).

465

A. Treatment Plan

B. Pretreatment

① Patient Setup and Localization

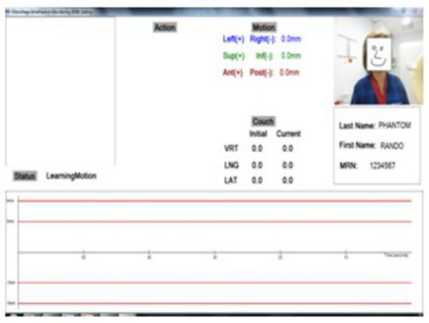

② KIM Software Activation

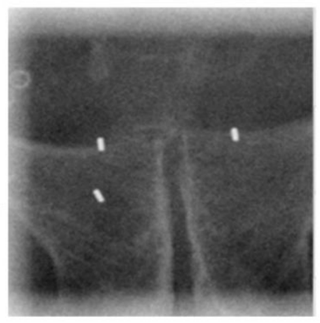

③ Acquire single kV image For CT verification

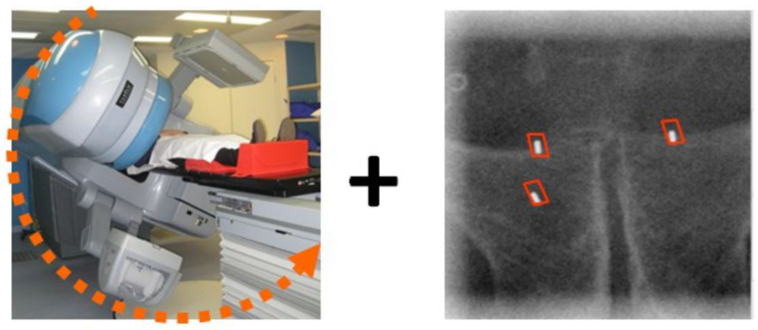

④ Pretreatment Arc Acquisition + Marker Segmentation

C. Treatment

⑨ MV Beam On

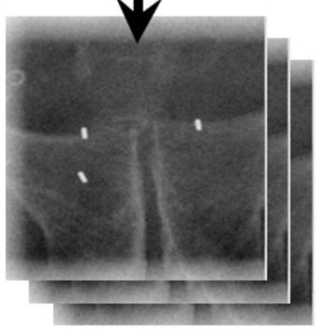

⑤ kV Acquisition

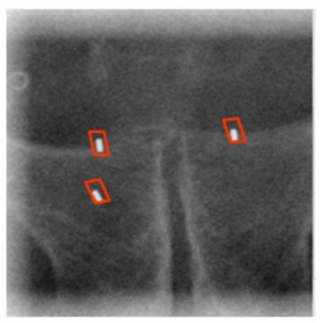

⑥ Marker Segmentation

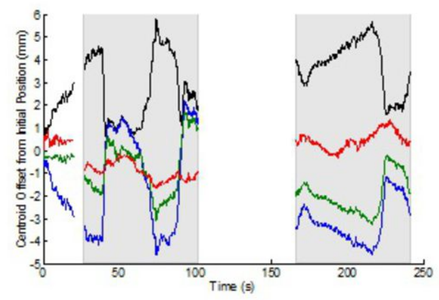

⑦ 3D Position Determination

⑧ Within Threshold?

YES

NO

⑩ MV Beam Off + Shift Couch

D. Post Treatment

⑪ KIM software deactivation

⑫ Store images and trajectories


TRILOGY

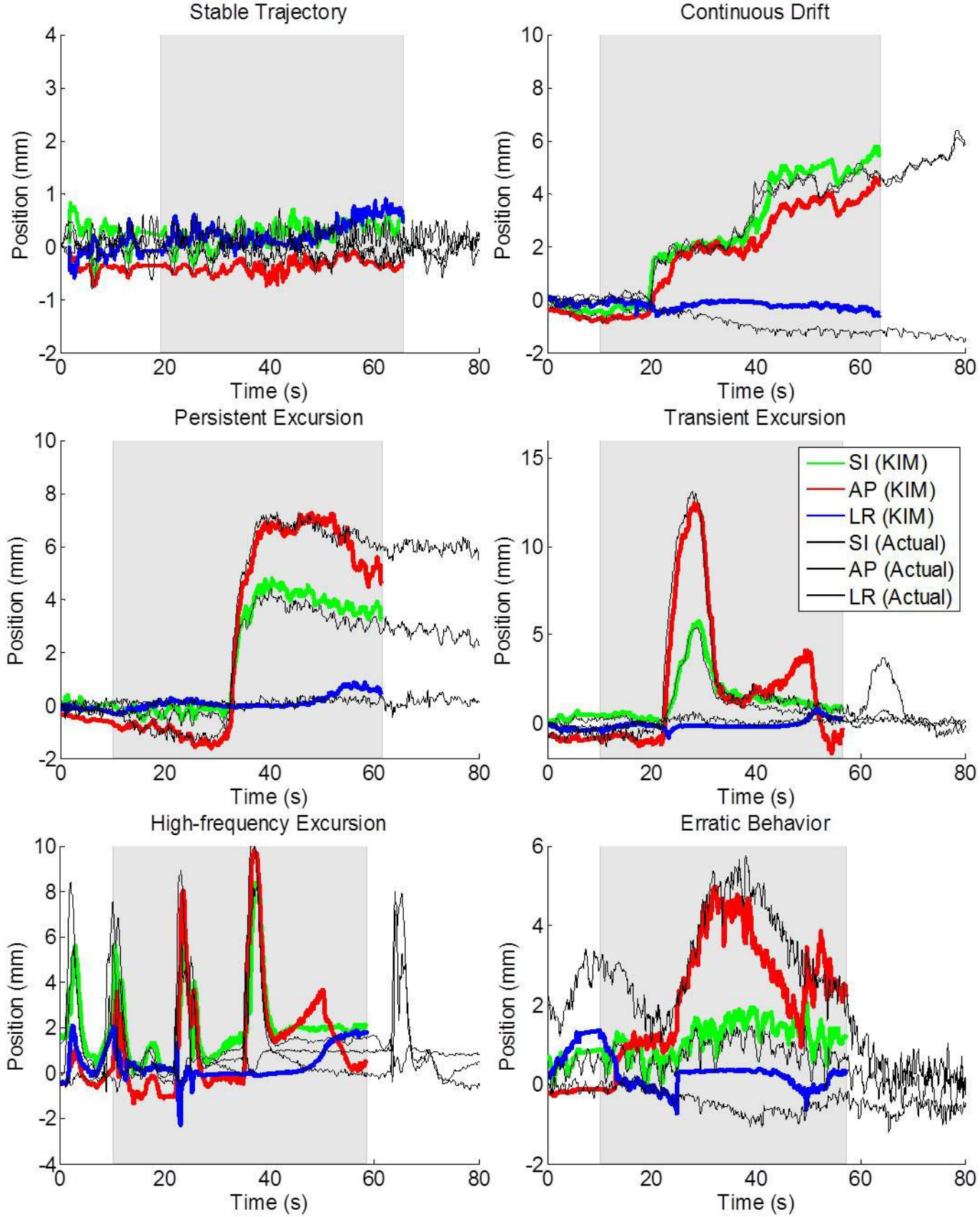
Stable Trajectory
Continuous Drift
Persistent Excursion
Transient Excursion
High-frequency Excursion
Erratic Behavior
Position (mm)
Time (s)
SI (KIM)
AP (KIM)
LR (KIM)
SI (Actual)
AP (Actual)
LR (Actual)

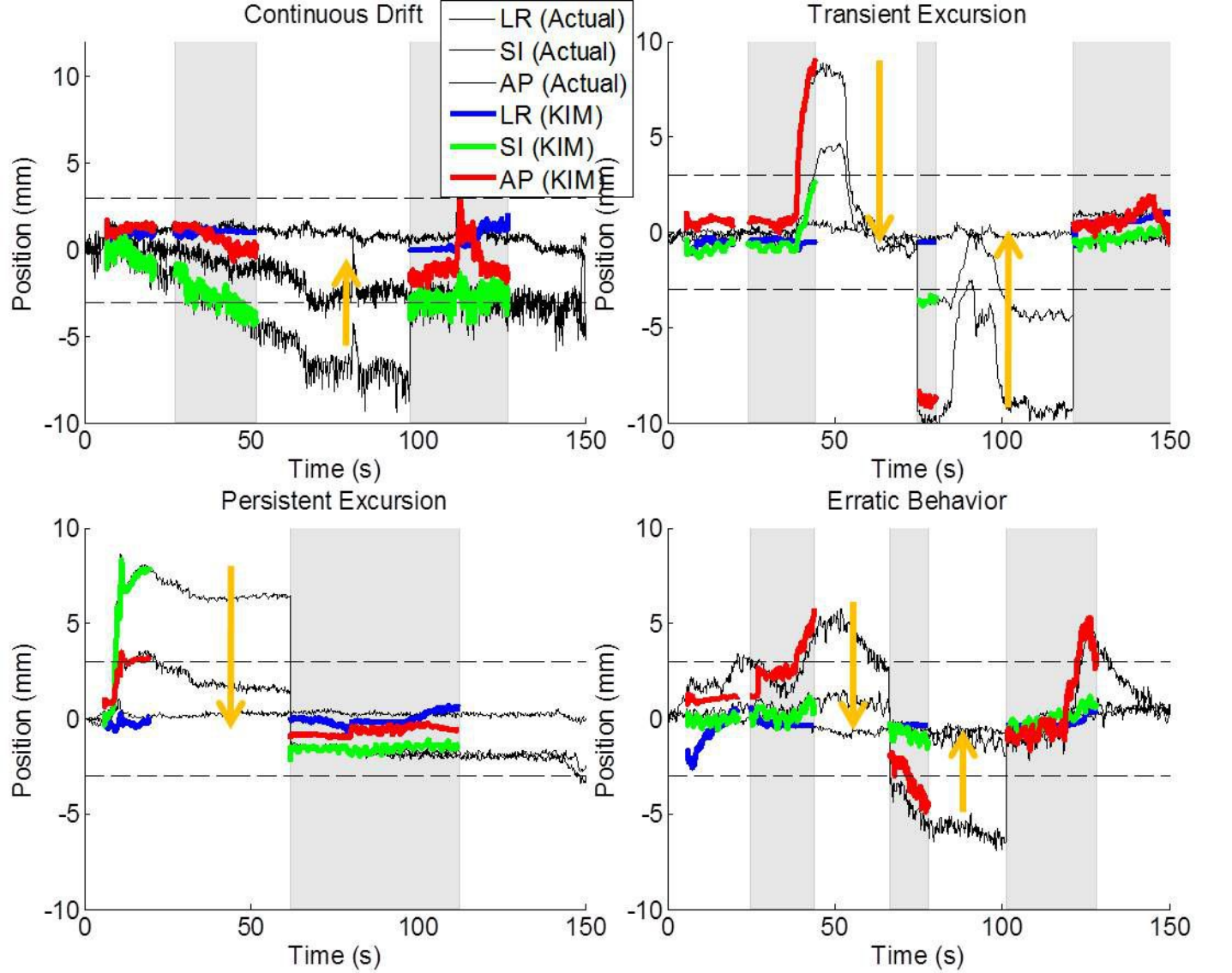
Continuous Drift
Transient Excursion
Persistent Excursion
Erratic Behavior
LR (Actual)
SI (Actual)
AP (Actual)
LR (KIM)
SI (KIM)
AP (KIM)
Position (mm)
Time (s)
10
5
0
-5
-10
0
50
100
150